

## PREDICTING FLEXURAL MODULUS OF ADDITIVELY MANUFACTURED CONTINUOUS CARBON FIBER-REINFORCED POLYMER COMPOSITES USING MACHINE LEARNING

**Ria Gandhi**  
University of Florida  
Orlando, FL

**Ziyang Zhang**  
University of Central  
Florida  
Orlando, FL

**Dazhong Wu**  
University of Central  
Florida  
Orlando, FL

### ABSTRACT

*Composites are labor-intensive and can be expensive to perfect on design and testing. Additive manufacturing (AM) processes are preferred over conventional fabrication methods. Carbon fiber-reinforced polymer (CFRP) composites are used because they are strong and light but it's difficult to estimate the mechanical properties of the AM parts. Data was collected from 10 specimens acquired from previous research and was programmed to output the necessary information as well as the flexural modulus. For future work, all specimens will be programmed to output the flexural modulus and will be put through machine learning algorithms in python to calculate outputs that are predicted accurately.*

### NOMENCLATURE

AM	Additive Manufacturing
CFRP	Carbon Fiber-Reinforced Polymer
FRP	Fiber-Reinforced Plastics
GFRP	Glass Fiber-Reinforced Plastics
FEA	Finite Element Analysis
CCFRP	Continuous Carbon Fiber-Reinforced
Polymers	
FDM	Fused Deposition Modeling
SVM	Supervised Learning Method

### 1. INTRODUCTION

The market is expected to reach over \$130 billion in size by 2024, this is due to a rapidly increasing demand in the aerospace industry for lightweight materials. These lightweight materials are composite materials, which allude to two or more constituent materials with different mechanical properties. Some mechanical properties include tensile strength, elasticity, fracture toughness, shear strength, flexural strength, and fatigue limit. Composites are often used to reduce weight because of their higher strength compared to traditional bulk materials such as metal matrix and ceramic matrix composites, reinforced concrete, and reinforced plastics. Composite materials are applicable in multi-disciplinary fields. Application of composites includes aerospace, architecture, automotive, energy, construction, healthcare,

infrastructure, marine goods, and transportation [1–4]. Boeing uses fiber-reinforced plastics (FRP) in the structure of the airframe and the Boeing 787 planes. Due to glass fiber-reinforced plastics (GFRP) having great corrosion resistance and high temperature resistance, they have been used in the fabrication of wind turbine blades. Mechanical properties such as malleable compressive, tensile, shear, and fracture strength of FRP have been studied since it is important to understand the design and fabrication of products [3,5]. The beam-shaped or plate-shaped composites, which exhibit in flexural behavior of FRP has not been studied yet [6,7]. Bending, a prime condition in the application of CFRP composites, was utilized in the manufacturing of the Boeing 787 wing structure and as a reinforcer on the B-pillar on the BMW 7-series [8].

Injection molding, resin transfer molding, layup, filament winding, and compression molding are some labor-intensive methods composites materials. Designing, testing, and tooling requirements of molds made of metallic materials is expensive. Additive manufacturing (AM) processes are considered to surpass the limits of composite methods. There are seven categories of AM techniques: binder jetting, directed energy deposition, material extrusion, material jetting, powder bed fusion, sheet lamination, and vat photopolymerization.

Uniquely, without requiring molding, AM can produce lightweight, geometrically lightweight parts. However, since CFRP composites depend on design factors, it is difficult to estimate the mechanical properties of AM parts [10-13]. While finite element analysis (FEA) has been used to model the mechanical behavior of additively manufactured parts, it is difficult to obtain a high fidelity FEA model to predict the mechanical properties of additively manufactured continuous carbon fiber-reinforced polymers (CCFRP) composites. For example, a high fidelity FEA requires proper modeling of interfaces between the matrix and reinforcement materials using fracture mechanics-based models such as the cohesive zone method. However, the development of a material property library, including the required interfacial fracture parameters, is very time-consuming.

This paper aims to develop a data driven modeling approach that predicts the flexural modulus of additively manufactured

CCFRP. The goal of this research is to exemplify the use of machine learning and the ability to predict the flexural modulus of CCFRP specimens with different design parameters.

**2. MATERIALS AND METHODS**

The purpose for this research project is to predict the flexural modulus of CCFRP composites using a data-driven modeling approach. This will also help understand the structure and importance of the CCFRP.

**2.1 Materials**

Researchers, previously, designed and fabricated 162 CCFRP specimens using fused deposition modeling (FDM) while taking into account the number of fiber layers, the number of fiber rings, and polymer infill patterns of the specimens. The reinforcing material was the continuous carbon fibers, and the matrix material was the short carbon fiber-reinforced nylon. The dimensions of the CCFRP specimens were 130 mm × 15 mm × 3.50 mm, were 28 layers each, with each layer being 0.125 mm thick.

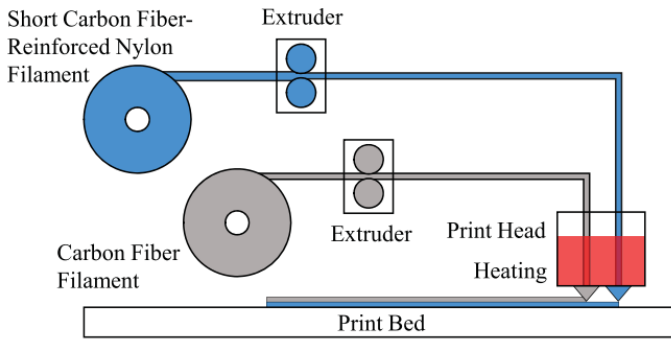


**Fig. 1 Schematic of the FDM process of CCFRP**

A commercial 3D printer (Markforged Mark Two, Watertown, MA) was used to print the specimens. The dual nozzle of the print head in Fig. 1 prints continuous carbon fiber and short carbon fiber-reinforced nylon filaments separately. The filaments are pulled into the extruder which feeds the material into the print head in the 3D printing process. Continuous carbon fiber is preheated to 250 °C and short carbon fiber-reinforced nylon filaments are pre-heated to 275 °C.

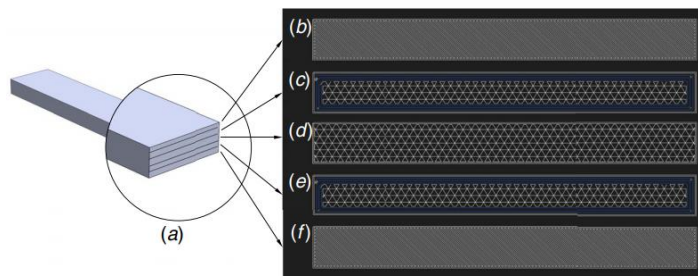


**Fig. 2 Schematic of the microstructure of a flexural test specimen. Outer lines represent concentric carbon fiber rings and inner triangles represent short carbon fiber-reinforced nylon: (a) layered CCFRP specimen, (b) top view of the cross section of roof layers, (c) top view of the cross section of carbon fiber-reinforced layers, (d) top view of**

**the cross section of polymer infill layers, (e) top view of the cross section of carbon fiber-reinforced layers, and (f) top view of the cross section of floor layers.**

Figure 2 displays the schematic of the microstructure of the specimen. The specimens contain three concentric carbon fiber rings and a triangular infill pattern. Figures 2(b)–2(f) show the top view of the cross sections of different types of layers. Figures 2(b) and 2(f) show the roof and floor layers. They are composed of four layers of solid short carbon fiber-reinforced nylon and fabricated at the top and bottom sections of the specimen. Figures 2(c) and 2(e) show the fiber layers. They are composed of concentric carbon fiber rings and sparse short carbon fiber-reinforced nylon with infill patterns. Figure 2(d) shows the polymer infill layers. They are composed of sparse short carbon fiber-reinforced nylon with infill patterns. Figure 3 shows the top views of the cross sections of layers with different polymer infill patterns. Outer lines represent concentric fiber rings and inner triangles represent short carbon fiber-reinforced nylon.

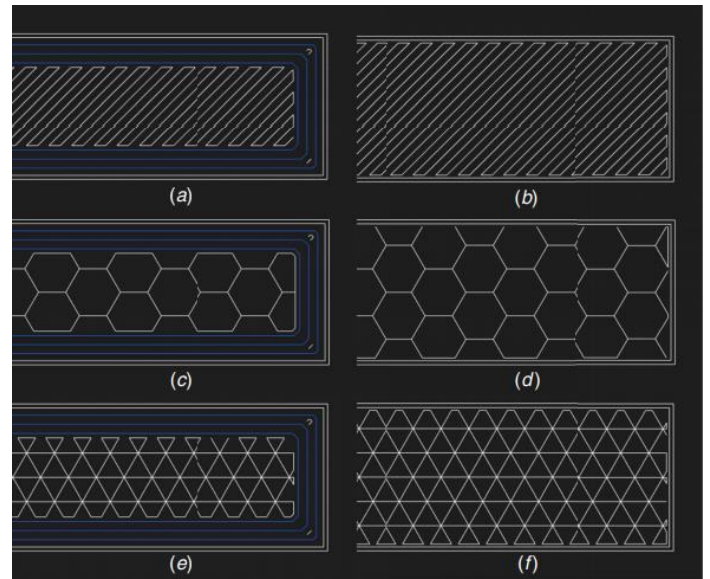


**Fig. 3 Different types of polymer infill patterns: (a) carbon fiber-reinforced layer with a rectangular infill pattern, (b) polymer infill layer with a rectangular infill pattern, (c) carbon fiber-reinforced layer with a hexagonal infill pattern, (d) polymer infill layer with a hexagonal infill pattern, (e) carbon fiber-reinforced layer with a triangular infill pattern, and (f) polymer infill layer with a triangular infill pattern**

Figures 3(a) and 3(b) show the fiber layers and polymer infill layers with a rectangular infill pattern. Figures 3(c) and 3(d) show the fiber layers and polymer infill layers with a hexagonal infill pattern. Figures 3(e) and 3(f) show the fiber layers and polymer infill layers with a triangular infill pattern.

**2.2 Design of Experiments**

Table 1 shows the experimental design. The experiment includes three design factors which are the number of fiber layers which has nine (9) levels, the number of fiber rings has six (6) levels, and the polymer infill pattern has three (3) levels. Both

levels of the number of fiber layers and the number of fiber rings are determined by the geometry of the specimen. The number of fiber layers are even because fiber layers are distributed symmetrically on top and bottom of a specimen. The three levels of the polymer infill pattern are rectangular, hexagonal, and triangular.

**Table 1 Design of Experiments**

Factor	Levels								
	1	2	3	4	5	6	7	8	9
Number of fiber layers	2	4	6	8	10	12	14	16	18
Number of fiber rings	1	2	3	4	5	6	NA	NA	NA
Polymer infill pattern	Rectangular	Hexagonal	Triangular	NA	NA	NA	NA	NA	NA

**2.3 Flexural Test**

The flexural properties of the CCFRP specimens were determined by four-point flexural tests according to ASTM D6272-17 [14]. The load span, *L*, was the support span. The flexural modulus of the samples was acquired from the flexural stress–strain curves.

**3. RESULTS AND DISCUSSION**

**3.1 Flexural Modulus**

To calculate the flexural stress and strain, the data reduction scheme was used from ASTM D6272-17. Flexural stress was calculated by

$$\sigma = \frac{3FL}{4bd^2}$$

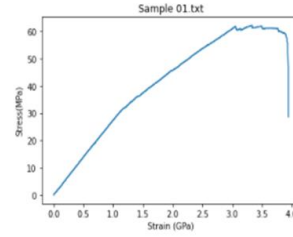
*F* is the measured force, *L* is the length of the support span, *b* is the sample width, and *d* is the sample thickness. The flexural strain was calculated by

$$\epsilon = \frac{4d\delta}{3L^2}$$

where  $\delta$  is the applied deflection.

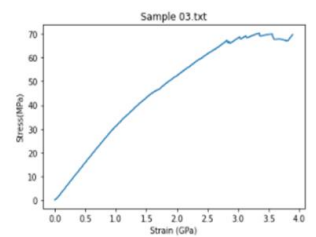
The stress and strain of the 10 specimens was calculated using the data reduction scheme shown above and was plotted into graphs from the load and extension. The flexural modulus was calculated from the data as well and was outputted below the graphs shown in Figures 4 – 8.

**Fig. 4 Graphs of specimen 1 and 2**

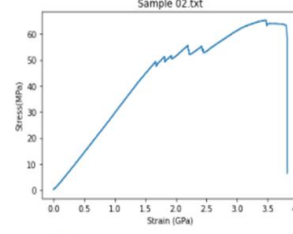


Slope 01.txt  
2.7308592079792305

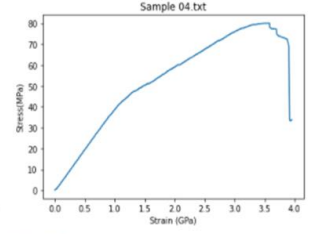
**Fig. 5 Graphs of specimen 3 and 4**



Slope 03.txt  
2.5157550243639064

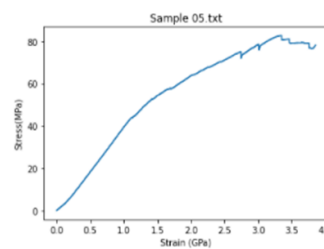


Slope 02.txt  
2.99985136900668



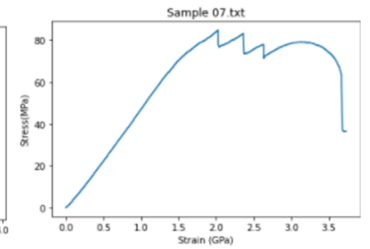
Slope 04.txt  
2.755787653391811

**Fig. 6 Graphs of specimen 5 and 6**

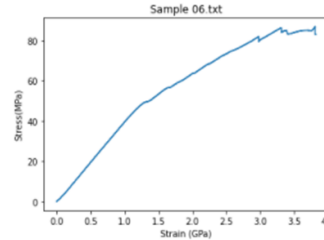


Slope 05.txt  
4.072986568164318

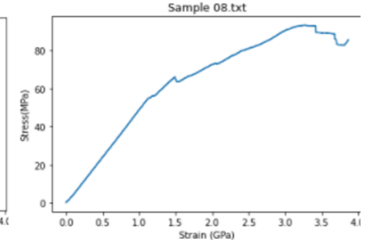
**Fig. 7 Graphs of specimen 7 and 8**



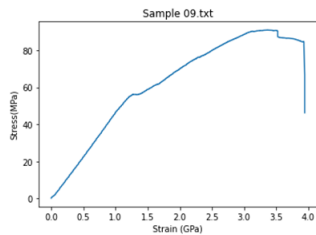
Slope 07.txt  
4.834114772219687



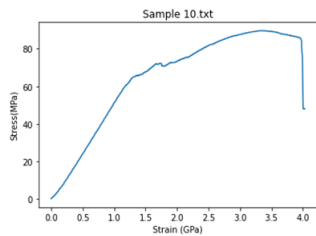
Slope 06.txt  
3.98682281111634



Slope 08.txt  
4.914779093957656

**Fig. 8 Graphs of specimen 9 and 10**

Slope 09.txt  
3.2937921022177528



Slope 10.txt  
3.500529469984577

#### 4. FUTURE WORK

For future work pertaining to this research project, 162 specimen data will be imported into Jupyter notebook. The graph for 162 specimens will be outputted. The flexural modulus will be calculated and outputted as well. Machine learning in python will then be implemented to take this data and will be split into training and testing data. They will then have put them through Xgboost, Randomforest, Ridge Regression, and Supervised Learning Method (SVM) algorithms and the parameters will be hyper tuned as needed to create an accurate prediction. The purpose of splitting up the data into training and testing data is so that the algorithm is trained through that percentage of data and tested through the other percentage of data and is able to calculate outputs that are highly predictively accurate. The use of the four different types of algorithms is used to compare them to each other and see which algorithms are more likely to accurately predict the outputs. For future use if there were specimens with different design factors, this algorithm could be used to accurately predict the flexural modulus.

#### ACKNOWLEDGEMENTS

This work was funded by the National Science Foundation and the Department of Defense. Acknowledgments also go to the Dr. Ali Gordan, Dr. Jeffrey Kauffman, Robert Burke, Dr. Dazhong Wu, and Ziyang Zhang.

#### REFERENCES

- [1] Wang, X., Jiang, M., Zhou, Z., Gou, J., and Hui, D., 2017, "3D Printing of Polymer Matrix Composites: A Review and Prospective," *Composites Part B*, 110, pp. 442–458.
- [2] Bakis, C. E., Bank, L. C., Brown, V., Cosenza, E., Davalos, J., Lesko, J., Machida, A., Rizkalla, S., and Triantafillou, T., 2002,

- "Fiber-Reinforced Polymer Composites for Construction—State-of-the-Art Review," *J. Compos. Constr.*, 6(2), pp. 73–87.
- [3] Kretsis, G., 1987, "A Review of the Tensile, Compressive, Flexural and Shear Properties of Hybrid Fibre-Reinforced Plastics," *Composites*, 18(1), pp. 13–23.
- [4] Ramakrishna, S., Mayer, J., Wintermantel, E., and Leong, K. W., 2001, "Biomedical Applications of Polymer-Composite Materials: A Review," *Compos. Sci. Technol.*, 61(9), pp. 1189–1224.
- [5] Machado, J., Marques, E., Campilho, R., and da Silva, L. F., 2017, "Mode II Fracture Toughness of CFRP as a Function of Temperature and Strain Rate," *Composites Part B*, 114, pp. 311–318.
- [6] Li, T., and Wang, L., 2017, "Bending Behavior of Sandwich Composite Structures With Tunable 3D-Printed Core Materials," *Compos. Struct.*, 175, pp. 46–57.
- [7] Keller, T., and Schollmayer, M., 2004, "Plate Bending Behavior of a Pultruded GFRP Bridge Deck System," *Compos. Struct.*, 64(3-4), pp. 285–295.
- [8] Wang, Z., Lauter, C., Sanitther, B., Camberg, A., and Troester, T., 2016, "Manufacturing and Investigation of Steel-CFRP Hybrid Pillar Structures for Automotive Applications by Intrinsic Resin Transfer Moulding Technology," *Int. J. Automot. Compos.*, 2(3-4), pp. 229–243.
- [9] Parandoush, P., and Lin, D., 2017, "A Review on Additive Manufacturing of Polymer-Fiber Composites," *Compos. Struct.*, 182, pp. 36–53.
- [10] Tian, X., Liu, T., Yang, C., Wang, Q., and Li, D., 2016, "Interface and Performance of 3D Printed Continuous Carbon Fiber Reinforced PLA Composites," *Composites Part A*, 88, pp. 198–205.
- [11] Li, N., Li, Y., and Liu, S., 2016, "Rapid Prototyping of Continuous Carbon Fiber Reinforced Polylactic Acid Composites by 3D Printing," *J. Mater. Process. Technol.*, 238, pp. 218–225.
- [12] Ning, F., Cong, W., Wei, J., Wang, S., and Zhang, M., 2015, "Additive Manufacturing of CFRP Composites Using Fused Deposition Modeling: Effects of Carbon Fiber Content and Length," *ASME 2015 International Manufacturing Science and Engineering Conference*, Charlotte, NC, June 8–12, American Society of Mechanical Engineers, p. V001T02A067.
- [13] Dickson, A. N., Barry, J. N., McDonnell, K. A., and Dowling, D. P., 2017, "Fabrication of Continuous Carbon, Glass and Kevlar Fibre Reinforced Polymer Composites Using Additive Manufacturing," *Addit. Manuf.*, 16, pp. 146–152.
- [14] ASTM International, 2017, D6272-17 Standard Test Method for Flexural Properties of Unreinforced and Reinforced Plastics and Electrical Insulating Materials by Four-Point Bending, ASTM International, West Conshohocken, PA.